

Comparative Study on the Wear Behaviour of Two High-Temperature-Resistant Polymers

Li Chang¹ · Ga Zhang² · Hongjian Wang¹ · Kunkun Fu¹

Received: 2 November 2016 / Accepted: 16 January 2017 / Published online: 27 January 2017
© Springer Science+Business Media New York 2017

Abstract The wear behaviour of two kinds of high performance polymers, i.e. polyetheretherketone (PEEK) and polybenzimidazole (PBI) was investigated at room and elevated temperatures (up to 175 °C). The results showed that PBI possessed better wear resistance than PEEK when the temperature was lower than 70 °C, which can be explained by the excellent thermal mechanical properties of PBI. However, PEEK showed even higher wear resistance when temperature is above 140 °C. It was noted that the formation of an effective TFL plays a key role in determining the wear performance of the polymer/steel system. In particular, the relatively low wear rate for PEEK achieved at elevated temperatures when the “transfer film efficiency factor” was clearly larger than one, although the mechanical properties of PEEK were significantly degraded. This means that under these conditions, the wear process of the polymer would be governed by the damage and regeneration process of the TFL at the interface rather than the bulk properties of the polymer specimen. The selection of high performance polymers for high wear resistance needs to consider not only their thermal mechanical properties, but also the possible wear regime(s) under the sliding conditions in the required applications.

Keywords High-temperature-resistant polymers · Tribology · Fracture · Transfer film layer

1 Introduction

Over the past decades, polymeric materials have been increasingly used as tribo-materials in the aerospace, automotive, and chemical industries, providing lower weight alternatives to traditional metallic materials [1–9]. A number of these applications are concentrated on tribological components such as gears, cams, bearings, and seals, where the self-lubrication of polymers is of special advantage. In particular, it has become a research trend to explore the potential of existing versus newly developed high performance polymers for special tribological applications in which reliable mechanical and tribological properties at high temperatures are desirable [10–15]. For instance, polymer-based materials have been used as control arm mountings or ball joints in the new car chassis technology and sliding shoes in textile drying machines where external liquid lubricants cannot be used due to the design and/or cleanliness requirements [7]. In these cases, polymeric materials have to operate as sliding or rolling elements at relatively high environmental temperature (e.g. up to 150 °C), and the demand for high wear resistance becomes increasingly important. High performance polymers such as polyetheretherketone (PEEK), polyimide (PI), and polybenzimidazole (PBI) are particularly interesting candidates for these applications [10, 16, 17].

Amongst these polymers, PEEK can be considered as a representative high performance polymer, possessing high temperature resistance, strong mechanical properties, and high chemical stability. Moreover, the tribological properties of PEEK materials can be further enhanced by using

✉ Li Chang
li.chang@sydney.edu.au

¹ Centre for Advanced Materials Technology, School of Aerospace, Mechanical and Mechatronic Engineering, The University of Sydney, Sydney, NSW 2006, Australia

² State Key Laboratory of Solid Lubrication, Lanzhou Institute of Chemical Physics, Chinese Academy of Sciences, Lanzhou, China

various tribo-fillers such as fibres and solid lubricants, which can be manufactured using conventional melt processing techniques, e.g. extrusion and injection moulding [7]. Up to now, PEEK and PEEK-based composite materials have been studied and used in a wide range of applications even under severe sliding conditions [10–12, 14, 15, 18]. It is generally agreed that the high thermal mechanical properties of PEEK contribute to its desirable tribo-performance. In particular, it was noticed that the higher toughness of PEEK normally favours a higher sliding wear resistance of the PEEK-based material against metals [10]. This somewhat agrees with the proposed relationship that abrasive wear of polymers is inversely proportional to the rupture stress or the rupture work (i.e. the product of the rupture stress and the associated strain) [19–21], which also highlights the shear/tensile nature of the failure process in wear [2].

More recently, PBI has received increasing attentions, as the highest performing engineering plastic currently available. The heat deflection temperature of PBI can be higher than 400 °C with mechanical property retention over 205 °C. The unique property profile of PBI also makes it as an ideal candidate for some special tribological applications. For example, PBI has been used as contact seals and insulator bushings in plastic production and moulding equipment, which is hardly replaced by any other engineering material owing to the strict requirements [17]. Up to now, the tribological properties of PBI have been studied under various wear modes [16, 22–25]. Häger [22] and Marx et al. [23] studied the wear behaviour of PBI as a bearing material. The results showed that PBI can achieve high wear resistance under a high pressure of 10 MPa and a sliding speed of 0.1 m/s, which is comparable to the PEEK composite reinforced by carbon fibres. However, the relatively high specific wear rate was noticed at high velocity, which was attributed to the cracks perpendicular to the direction of sliding [23]. Lu et al. [24] confirmed the excellent tribological performance of PBI at room temperature and elevated temperatures up to 200 °C, which were tested on a ball-on-disk machine with a sliding velocity of 0.20 m/s and a load of 10 N. However, the wear rate sharply increased when the temperature became higher than 220 °C. It was explained that PBI was softened at high temperatures and thus more easily abraded. Pei et al. [16] compared the sliding wear properties of PBI, PEEK and PPP tested on a pin-on-disk configuration. The results indicated that PBI shows the highest wear resistance at ambient temperature when the pv factor varied from 0.5 to 4.6 MPa m/s. Sharma et al. [25] studied the sliding and erosion wear of PBI at different temperatures. It was concluded that the sliding and erosion wear rate of PBI

generally increased at elevated temperatures, since the mechanical properties of the material are moderately reduced with temperature.

The brief review demonstrates the strong potential of such high-temperature-resistant polymers for tribological applications even under extreme sliding conditions. The resultant high wear resistance of these polymers has been generally attributed to their high thermal mechanical properties. Nevertheless, tribological behaviour is not an intrinsic property of the materials, but depends on the system within which the material has to function. Under different wear conditions, the tribological performance of the material may be determined by the different combinations of properties due to the changes in the governing wear mechanism [26], which, however, has not been investigated in depth for such high performance polymers.

2 Materials and Experimental

2.1 Materials

Two high performance polymers, i.e. PEEK and PBI, were selected for this study. PEEK samples were prepared in-house using an Arburg injection moulding machine. PBI samples were received from the manufacturer (PBI Performance Products, Inc., Charlotte, NC, USA, type Celazole U60SD) as compression moulded (sintered) plates. Then, the specimens were further machined into specific geometries, according to the requirements for mechanical and tribological testing.

2.2 Characterization of Mechanical Behaviour

To understand the behaviour of polymers at different temperatures, the thermal–mechanical properties of the two polymers were characterized via a dynamic mechanical thermal analyser (DMTA) (Eplexor, GABO QUALIMETER Testanlagen GmbH, Ahlden, Germany), under tension configuration. The complex modulus and loss factor of each specimen ($55 \times 10 \times 2 \text{ mm}^3$) were determined at a constant frequency of 10 Hz, raising the temperature from room temperature to 250 °C for PEEK and 500 °C for PBI samples, at a heating rate of 1 °C/min.

Further, quasi-static tensile fracture tests were conducted at different temperatures using compact tension (CT) specimens. The tests were carried out using a Zwick 1485 universal testing machine, following the standard ISO 13586. The dimensions of the CT specimens were $4 \times 30 \times 30 \text{ mm}^3$ for PEEK and $6 \times 26 \times 26 \text{ mm}^3$ for PBI. A pre-crack was made by lightly tapping a fresh razor blade into the bottom of the saw slot in the specimen, in order to create a sharp natural crack. All the

tensile tests were performed at a crosshead speed of 10 mm/min.

2.3 Wear Characterization

The wear tests were carried out with a Wazau pin-on-disc apparatus according to ASTM D3702. The square cross section of the specimen pin ($4 \times 4 \times 12 \text{ mm}^3$) was run against a polished steel disk with an initial surface roughness of 220 nm, using a contact pressure of 1 MPa and a sliding velocity of 1 m/s. To evaluate the durability of the materials at elevated temperatures, the steel disk was heated and the temperature controlled by a heating device. During the test, the actual test temperature was monitored by an iron-constantan thermocouple positioned on the edge of the disk. The friction coefficient was recorded and calculated by the ratio between the tangential force and the normal load. The reduction in the height of the specimen, measured by a displacement transducer, could be used to characterize the wear process. However, the reliability of the measurement was affected by the possible thermal expansion of the sliding counterparts. Therefore, the mass loss of the specimen was also measured to calculate the specific wear rate by the equation,

$$W_s = \frac{\Delta m}{\rho F_N L} \quad (\text{mm}^3/\text{N m}) \quad (1)$$

where Δm is the mass loss of the specimen, ρ is the density of the specimen, F_N is the load applied on the specimen during sliding, and L is the total sliding distance. After the wear test, the worn surfaces and the wear tracks on the steel counterparts were examined using both scanning electron (SEM; JEOL 5400) and optical microscopy (Leica light microscope).

2.4 Nanoindentation Tests

The nanoindentation experiments were conducted to measure the hardness of the worn surfaces, using a nano-tri-indentation device (Hysitron Inc., USA) with a Berkovich indenter. All the indentation tests were carried out at a peak load of 3 mN, with the loading/unloading rate of 0.3 mN/s. A holding time of 5 s was applied at the maximum load to minimize time-dependent creep effects. Moreover, the indentation tests were also carried out to quantitatively characterize the transfer film layers (TFL) on the steel counterface. In this case, the TFL can be treated as a soft thin film on a hard substrate. The thickness of the TFL can be estimated by studying the load–displacement behaviour of the TFL on the basis of a relatively simple model. The detailed analysis can be found in our previous work [27]. It has been shown that the thickness of the TFL can be estimated by the equation,

$$h_f = h_t - h_s = h_t \left(1 - \frac{h_s}{h_t} \right) = h_t \left(1 - \sqrt{\frac{H_C - H_f}{H_S - H_f}} \right) \quad (2)$$

where h_f is the film thickness, h_t is the total indentation depth, and h_s is the indentation depth in the substrate. H_C is the measured composite hardness of the film/substrate system. H_f and H_s are the intrinsic hardness of the film and substrate, respectively. Although the calculation is based on a simplified contact model which may somewhat limit the accuracy of the calculated thickness, the analysis provides a practical way to quantitatively describe and compare the TFLs formed by various materials under different sliding conditions [27]. Further, with the thickness of TFLs, the “transfer film efficiency factor”, λ , can be determined by,

$$\lambda = \frac{t}{R_a} \quad (3)$$

where t is the average thickness of the TFL determined by nanoindentation tests, and R_a is the surface roughness of the steel counterface. The factor λ mainly considers the relative contributions of the TFL and the metallic counterpart to the wear process of the sliding system, i.e. a larger value of the factor indicates that the friction behaviour of the sliding system is more governed by the properties of the TFL.

3 Results

3.1 Thermal–Mechanical Properties and Fracture Toughness

Figure 1 gives DMTA results for the two polymers investigated. PEEK showed a storage modulus of $\sim 3 \text{ GPa}$ at

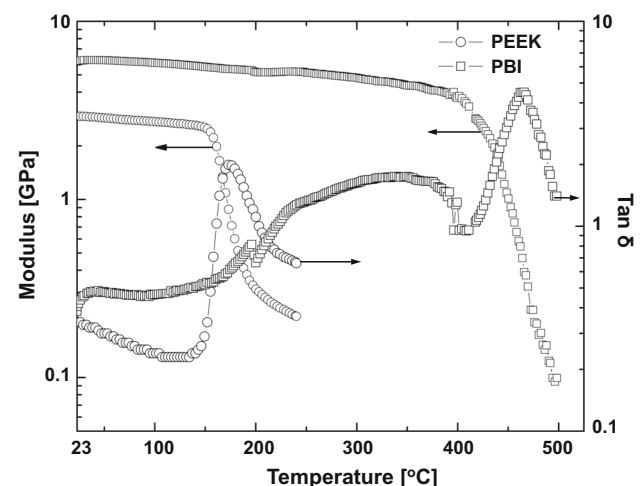


Fig. 1 Dynamic thermal mechanical properties of PEEK and PBI in a temperature range from room 23–250 and 500 °C, respectively

room temperature, which continuously decreased down to ~ 2 GPa at 140°C , before it sharply dropped in the range of the glass transition temperature. PBI, on the other hand, possessed a much higher storage modulus at room temperature (~ 6 GPa) and retained it at a relatively high value up to $\sim 400^\circ\text{C}$ (~ 4 GPa), thanks to its very high glass transition temperature.

To further understand the failure behaviour of the two polymers, fracture tests were conducted with CT samples at elevated temperatures. The typical tensile load–strain curves are given in Fig. 2. Accordingly, Fig. 3 summarizes the measured fracture toughness values. The results for PEEK were compared with the data reported by Karger-Kocsis et al. [28], which showed a good agreement. The fracture toughness of the material dropped from 6 to $1.5\text{ MPa m}^{1/2}$ when temperature increased up to 220°C , and the most dramatic decrease takes place within the range of the glass transition temperature. It should be stated that the size criteria for PEEK samples could not be fulfilled, which means that the measured K_{c} values are actually greater than those strictly determined under the plane strain condition. Here, the fracture energy was simply estimated from the 95% secant load [28]. It is noticed that at high temperatures, the material failed with large plastic deformation rather than by brittle fracture, owing to the low yielding stress or the softening of the polymer.

PBI showed more stable fracture behaviour within the tested temperature range, thanks to its extremely high temperature resistance. The samples mostly behaved in a brittle manner with the strains at the maximum load less than 1%. The measured K_{c} values slightly dropped from 3.5 to $2.8\text{ MPa m}^{1/2}$ when the temperature was increased from room temperature to 220°C . It is assumed that the thermal–mechanical properties of the polymers and their

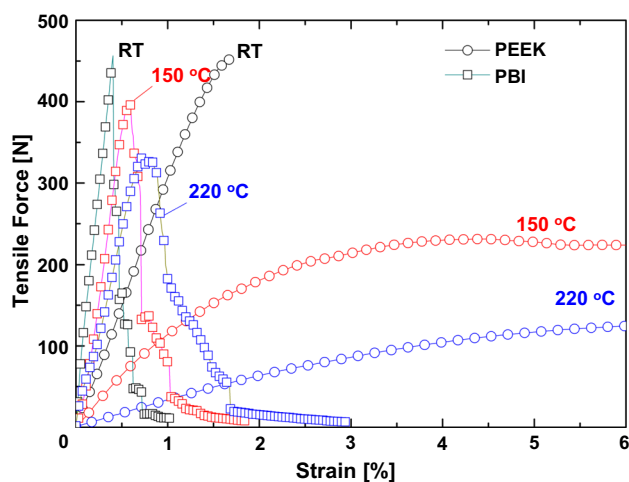


Fig. 2 Typical load–strain curves for PEEK and PBI from CT fracture tests at different temperatures, i.e. room temperature (RT), 150 and 220°C

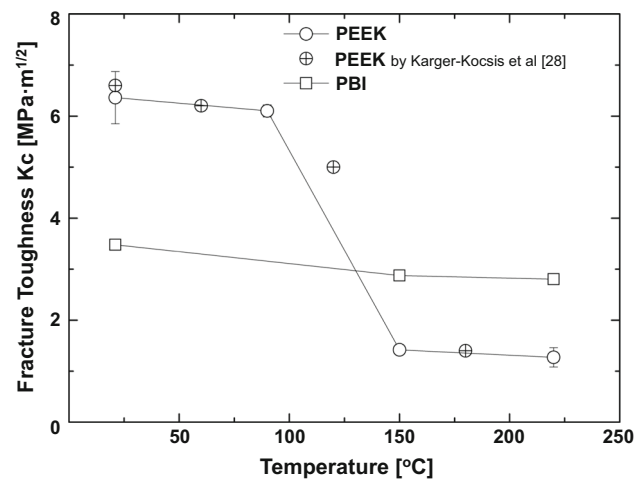


Fig. 3 Fracture toughness of PEEK and PBI as a function of temperature

fracture behaviour also affect directly their tribological performance, especially at high temperatures, which will be further discussed in the following section.

3.2 Wear Behaviour at Elevated Temperatures and Its Dependence on Other Mechanical Properties

Figure 4 compares the wear results for PBI and PEEK tested at different temperatures. PBI clearly shows better wear performance within a temperature range from room temperature to 140°C . However, PEEK tends to give a lower wear rate but higher friction coefficient at even higher temperatures. Similar tendencies have been also observed for PEEK specimens by Häger [29], although detailed mechanisms were not discussed. To understand the governing wear mechanisms at different temperatures, the worn surfaces of two polymers were further examined and compared.

As shown in Fig. 5a, b, at the room temperature, both PBI and PEEK obtained the relatively smooth worn surfaces with a small amount of wear particles and fine grooves, indicating that the wear process was governed by a mild abrasive wear mechanism caused by hard asperities of the steel counterpart. It is known that the abrasive wear rate of polymeric specimens is mostly dependent on its hardness, as described in the original Archard model [30]. The model is based on the assumption that wear occurs at the interface, and the wear volume by a single asperity tip is dependent on the plastic deformation depth on the specimen. Figure 6 compares the surface hardness of two polymers after the wear tests at different temperatures. It is worthwhile noting that the measured hardness of the worn surface of PEEK at room temperature agrees well with previous results for the original untested material, i.e.

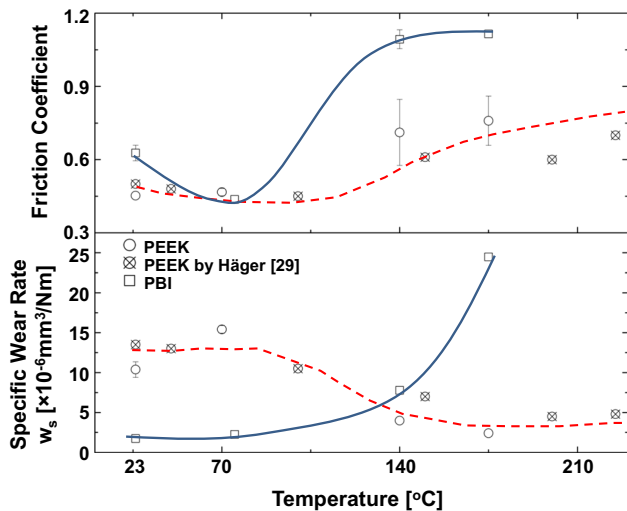


Fig. 4 Wear test results of PEEK tested at different temperatures. *Dashed lines* wear results of neat PEEK. *Solid lines* wear results of neat PBI. Sliding condition: 1 MPa, 1 m/s (some scatter bars are not shown in the figure, as they are smaller than the size of the symbols)

275 MPa, reported by Zhang et al. [31]. With the increase in temperature, the hardness of the worn surfaces steadily decreases, suggesting a more severe degradation of the polymer at higher temperatures. The measured hardness can be also affected by the existence of the transfer polymer and degraded polymer particles due to chemical wear. Nevertheless, it is clear that the hardness of PBI is always more than $2\times$ higher than that of PEEK after all the wear tests, which explains the higher wear resistance achieved by PBI at relatively low temperatures.

At 175 °C, however, the worn surfaces of two polymers showed distinctive characteristics. As shown in Fig. 7a, the scale of surface damage for PBI specimen significantly increased and occasional bulk failure was observed. It is also noticed that when testing temperature is higher than

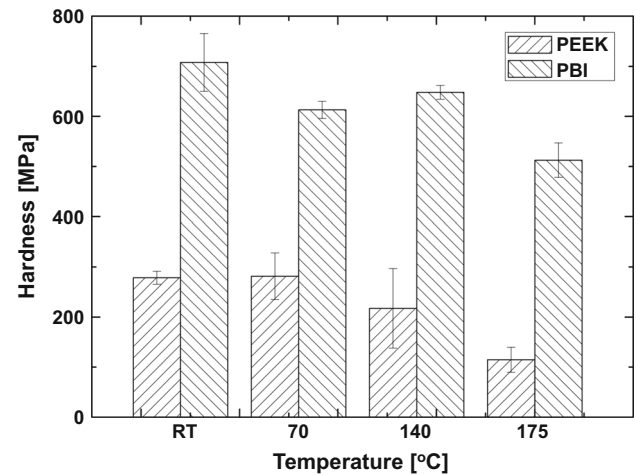


Fig. 6 Measured hardness of the worn surfaces of PBI and PEEK formed at different temperatures

170 °C, a blue oxide layer on the stainless steel counterpart could be seen, as reported by Häger et al. [22]. The oxide layer would not only enhance the surface hardness of the steel counterpart, but also significantly reduce its thermal conductivity. Consequently, more frictional heat fluxed into the PBI sample causing a high surface temperature. This would greatly weaken the connections of the sintered powder pieces. With the loosed powders in PBI, crack initiation and propagation took place in the surrounding regions due to the thermo-mechanical fatigue. As shown in the figure, the cracks are perpendicular to the sliding direction, which typically occurs under fretting-fatigue and fretting-wear contact conditions [32]. Such cracks were also observed in PBI [23] and ZnO filled polytetrafluoroethylene (PTFE) [33] specimens under sliding contacts. The continuing wear process produced numerous cracks at the surface associated with large wear particles. Further, the small dimensions of the specimens also allowed an easy

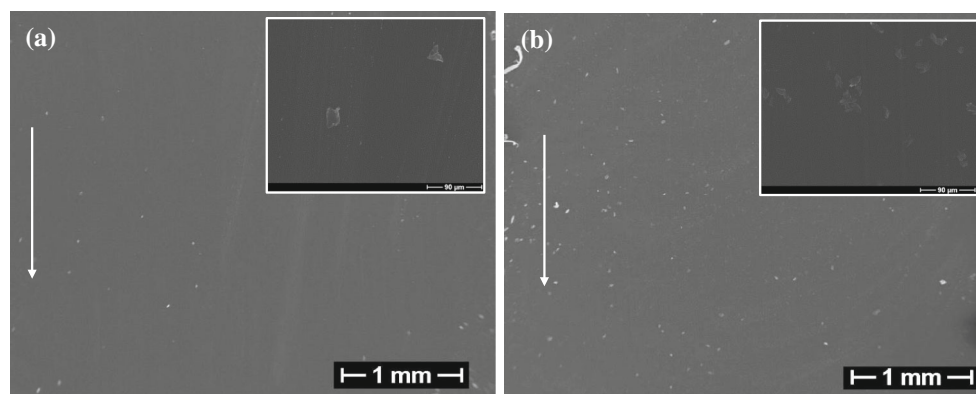


Fig. 5 SEM images of the worn surfaces of **a** PBI, **b** PEEK tested at room temperature. The sliding directions were indicated by the arrows

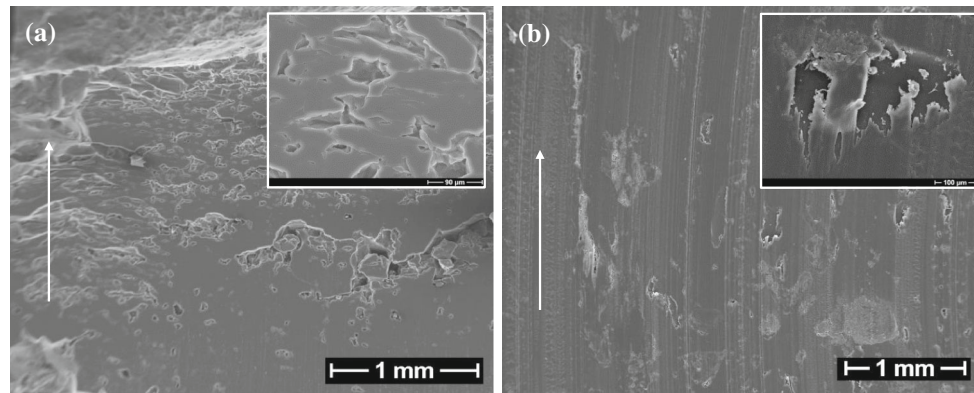


Fig. 7 SEM images of the worn surfaces of **a** PBI, **b** PEEK tested at 175 °C. The sliding directions were indicated by the arrows

breaking away of the edges of the quasi-brittle PBI (upper part of the worn PBI pins shown in Fig. 7a), resulting in the high wear rate at high temperatures.

For the PEEK specimen, at 175 °C, the worn surface is almost fully covered by the back-transferred wear debris, which was stretched and smeared out, resulting in a nearly continuous film (cf. Fig. 7b). Such a back-transfer film also suggests the existence of a transfer film layer (TFL) on the metal counterface. As shown in Fig. 8, the surface of the steel counterpart (before wear: Fig. 6a) was only slightly changed after the wear test at room temperature (Fig. 6b). At 175 °C, the surface was almost fully covered by the TFL, with grooves along the sliding direction (Fig. 7c). During sliding, wear mainly occurred at the interface between polymer layers, resulting in an adhesive or transfer wear mechanism. The grooves may be caused by the hardened wear debris. In this case, the wear performance of the sliding system would be less affected by the bulk properties of polymers, but mostly determined by the third body between the worn surfaces [34, 35]. In particular, the back-transfer film also suggested that the wear debris was effectively trapped in the wear region between the rubbing surfaces, which explains the very low wear rate of the PEEK specimens at higher temperatures. For comparison, Fig. 9 shows the microscopic observations of the wear tracks on the steel counterparts resulted from PBI specimens. It was found that PBI could not develop an effective TFL to fully cover the counterface under all the tested conditions. During the sliding process, abrasion wear always prevails due to the inevitable direct contact between the polymer specimen and the hard steel counterpart. Thus, the very low wear rate of PBI under mild ambient conditions was mainly attributed to its excellent mechanical properties, especially the very high hardness associated with a good resistance to fracture. However, the brittle nature of the material raises risks of severe surface damage and wear loss owing to the fracture failure under extreme sliding conditions.

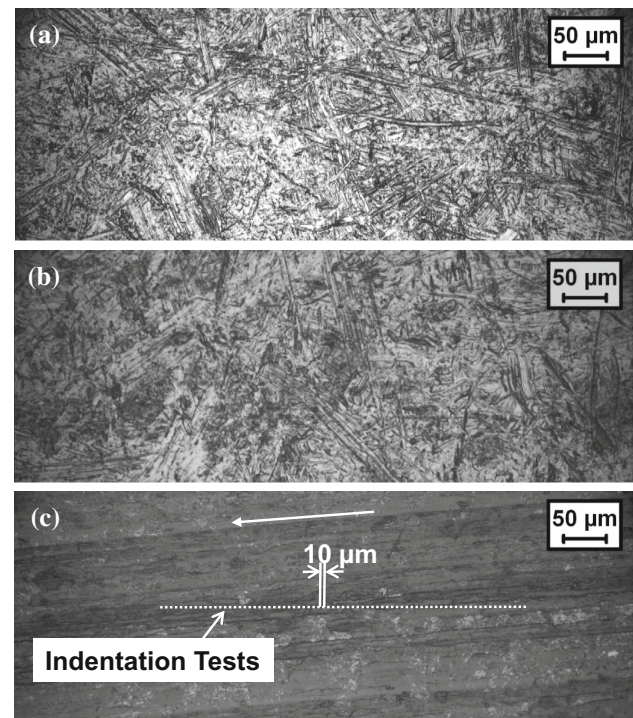


Fig. 8 Optical microscopy images of **a** the original surface of the steel disk, and the wear tracks on the steel counterface against PEEK specimens tested at different temperatures, **b** room temperature, **c** 175 °C. The sliding directions were indicated by the arrows

3.3 Development of the Polymeric TFLs on Steel Disks

The wear results and the SEM observations highlighted the important role of TFLs in determining the wear performance of polymers. To further study the tribo-effects of the TFL in tribological contacts and the mechanism of TFL development, the nanoindentation technique was adopted to obtain more reliable data of TFLs [27, 36, 37]. As shown in Fig. 8c, a number of indentation tests were continuously

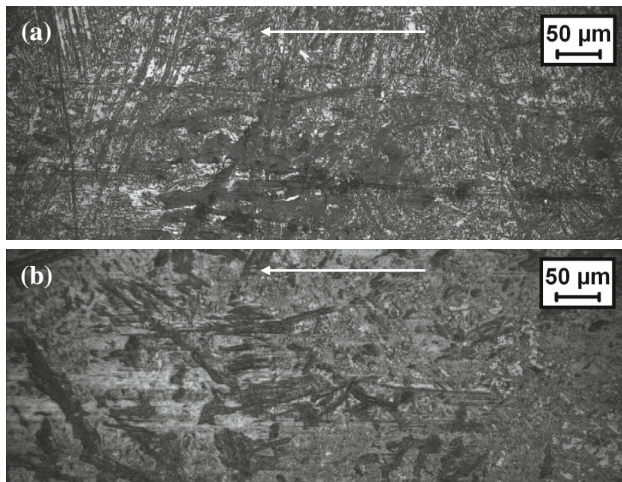


Fig. 9 Optical microscopy images of the wear tracks on the steel counterface against PBI specimens tested at different temperatures: **a** room temperature, **b** 175 °C. The *sliding directions* were indicated by the *arrows*

conducted along a crossline on the wear track, with a constant distance of 10 μm. Applying Eq. 2, the thickness of the localized TFL can be estimated from the indentation test. Then, the “average thickness” of the TFL could be determined by the mean value from 100 indentations.

Figure 10 shows the indentation results for the TFLs formed by PEEK at different temperatures. It is well confirmed that PEEK specimens could develop more effective TFLs at relatively high temperatures. It is interesting to note that the transfer film efficiency factor, $\lambda > 1$ when the temperature is higher than 140 °C, corresponding to the lower wear rates. This means the TFL can effectively cover the asperities of the original surface of the steel

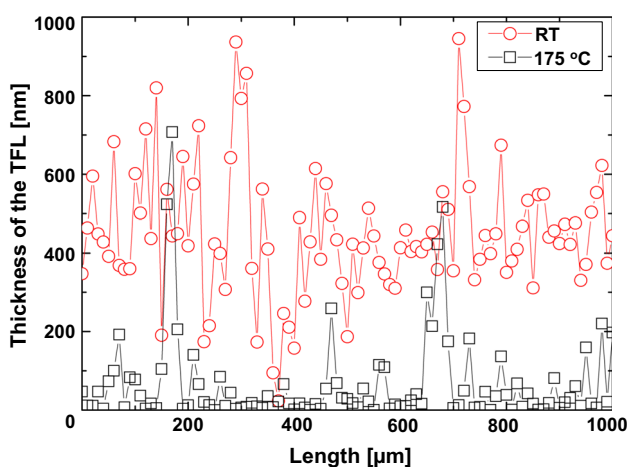


Fig. 10 Thickness distribution of the TFL developed by PEEK specimens tested at different temperatures. The mean values for the thickness of the TFLs are 67 nm (SD = 117), 91 (SD = 232), 393 (SD = 291) and 449 nm (SD = 165 nm) for the wear tests at RT, 70, 140 and 175 °C, respectively. *SD* standard deviation

counterpart, resulting in the three-body adhesive/transfer wear instead of two-body abrasive wear. The results also support the hypothesis that semi-crystalline polymers can develop a stable TFL on a metallic counterface and sometime a back-transfer film on the worn surface of the specimen, especially when the contact temperature reaches its glass transition temperature [34, 38].

The tribo-effects of the TFL can be further illustrated by the variations of friction coefficient and height loss of specimens against sliding time, as given in Fig. 11. The inserted numbers refer to the slopes of the height loss curves in the steady stage, i.e. the height loss rate of the specimens. These results are in a reasonable agreement with the wear rates determined by the mass loss given in Fig. 4 (since all the tests were carried out at 1 MPa m/s, a slope of 1 nm/s is equivalent to $1 \times 10^{-6} \text{ mm}^3/\text{Nm}$). As shown in the inserted figure in Fig. 11, at 175 °C, the PEEK specimen showed a much higher wear rate in the first 1 h, which is close to that at 70 °C. Then, the slope, i.e. the wear rate, gradually decreased and finally reached a much smaller, stable value of $\sim 2 \text{ nm/s}$. This means, in the running-in phase, the governing wear mechanism was changed due to the formation of the TFL. Figure 12 shows the development of the TFL on the steel disk in the first 2 h, compared with the worn surfaces of PEEK specimens. After 20 min, there are only few isolated patches of the TFL. Accordingly, deep grooves were observed on the

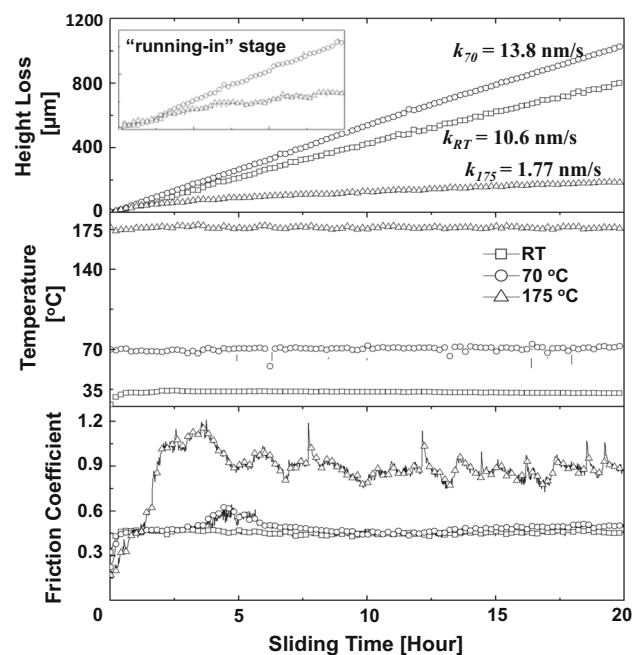


Fig. 11 Typical sliding performance of PEEK tested at different temperatures. The *inserted image* is a magnified view of the height loss curves in first 3 h obtained at 70 and 175 °C. The *inserted numbers* indicate the slopes of the height loss lines in the steady stage. Sliding condition: 1 MPa, 1 m/s

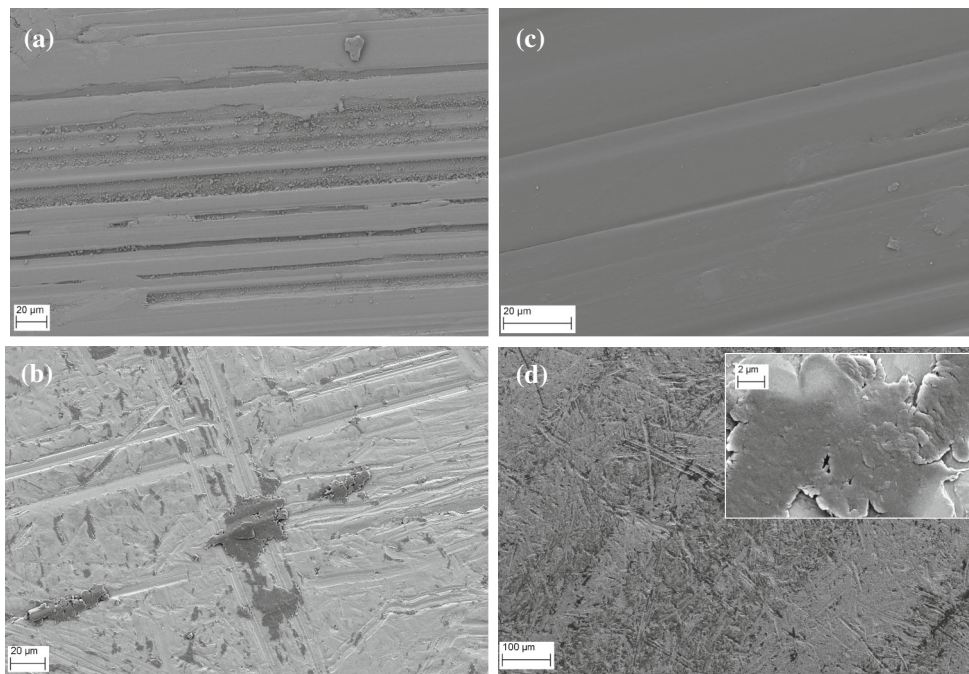


Fig. 12 SEM images of **a** the worn surfaces of PEEK, **b** the formation of the TFL on the steel counterpart after 20 min, **c** the worn surfaces of PEEK, **d** the formation of the TFL on the steel counterpart after 2 h

worn surfaces caused by two-body and three-body abrasive wear. Two hours later, however, the TFL became continuous, corresponding to a much smoother worn surface. The inserted image shows that formation of the TFL due to the plastic deformation of wear debris. Hence, it is proposed that the effect of temperature on the formation of the TFL is related to the brittle-ductile transition taking place in the glass transition range (cf. Figs. 1, 2). During the wear process, the transition led to the large plastic deformation of wear debris which formed with sheets or layers at high temperatures instead of fine powder-like particles at room temperature (Fig. 5). The former ones normally favour the formation of a TFL [4]. With a continuous TFL, the wear process in steady stage would be governed by the adhesion/transfer wear mechanism, resulting in a stable, lower wear rate. On the other hand, the friction coefficient in the steady stage was relatively high, due to the strong adhesive force between the transfer film layers on the worn surface and the steel counterface [6]. It should be noted that the fluctuations in friction coefficient cannot be explained by the stick–slip behaviour of polymers, which would happen in a much more frequent manner. The fluctuations in friction coefficient here are therefore caused by damage and regeneration of the TFL.

Figure 13 presents indentation results for the TFLs formed by PBI. The thickest TFL was formed at room temperature, with an average thickness of 172 nm, which is smaller than the surface roughness of the steel disk. Moreover, compared with the TFL formed by PEEK at

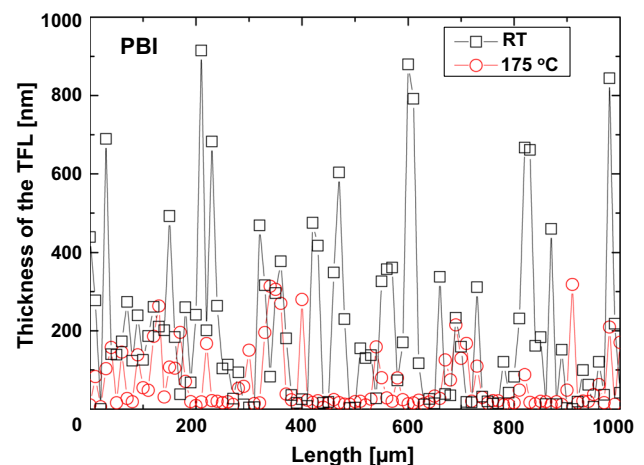


Fig. 13 Thickness distribution of the TFL developed by PBI specimens tested at different temperatures. The average values for the thickness of the TFLs are 172 nm ($SD = 181$), 44 ($SD = 81$), 42 ($SD = 65$), and 65 ($SD = 79$ nm) for the wear tests at RT, 70, 140, and 175 °C, respectively. *SD* standard deviation

high temperatures (e.g. at 175 °C shown in Fig. 10), the TFL formed by PBI at room temperature showed a poor uniformity with the thickness sharply varying from zero to ~ 1 μm . This means that there are only some isolated, compacted wear debris rather than an effective, continuous film in the contact region. Figure 14 shows the variations of frictional coefficient and height loss of PBI specimens against sliding time at different temperatures. It is noticed that the height loss rate remains stable during the whole

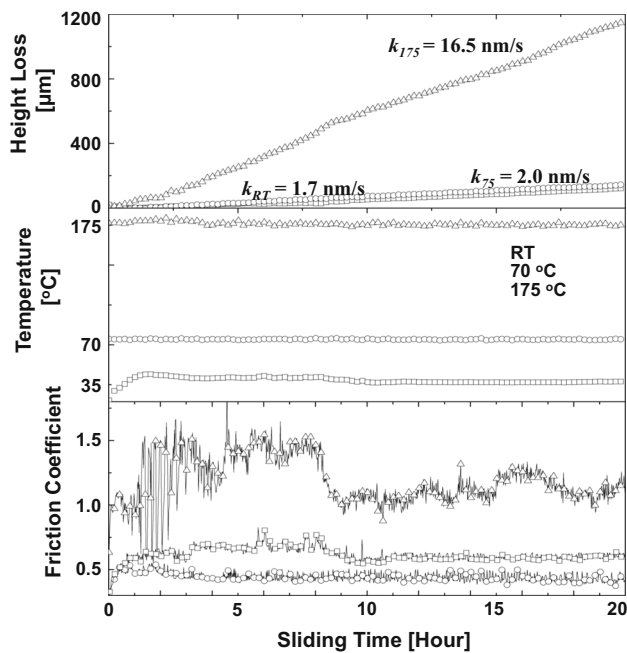


Fig. 14 Typical sliding performance of PBI tested at different temperatures. The *inserted numbers* indicate the slopes of the height loss lines in the steady stage. Sliding condition: 1 MPa, 1 m/s

wear process, suggesting that there is no obvious wear mechanism transition in the initial sliding stage, comparing with the results from PEEK (Fig. 11). The values of the height loss rate also agree reasonably with the wear rates determined by the mass loss.

The development of the TFL from PBI was further investigated during the running-in stage. As shown in Fig. 15b, even at high temperatures, the sub-micro and micro-sized particulate wear debris was generated in the early running-in stage because of the brittle failure behaviour of the material. The grooves were noticed on the worn surface, associated with few cracks perpendicular to the sliding direction (Fig. 15a). After 2 h, it can be seen the wear particles were compressed and filled in surface valleys (Fig. 15d). As a result, the surface roughness of the steel disk was effectively reduced, contributing to a smoother worn surface (Fig. 15c). Meanwhile, the smooth contact surfaces also cause a higher friction force (cf. Fig. 14), and consequently, the severe surface damages with more cracks. As the wear process continues, larger pieces of wear debris can get detached from the worn surface due to a coalescence of the fatigue cracks (cf. Fig. 7a). The removal of large pieces of debris may explain the sudden drop in friction coefficient after ~ 8 h shown in Fig. 14, due to a reduction in the contact area. This also explains the higher wear rate at 175 °C determined by the mass loss, compared with that measured by the geometric height reduction.

4 Discussion

In this paper, we studied and compared the wear results for two high performance polymers tested on a pin-on-disk configuration. The results showed that without the effective

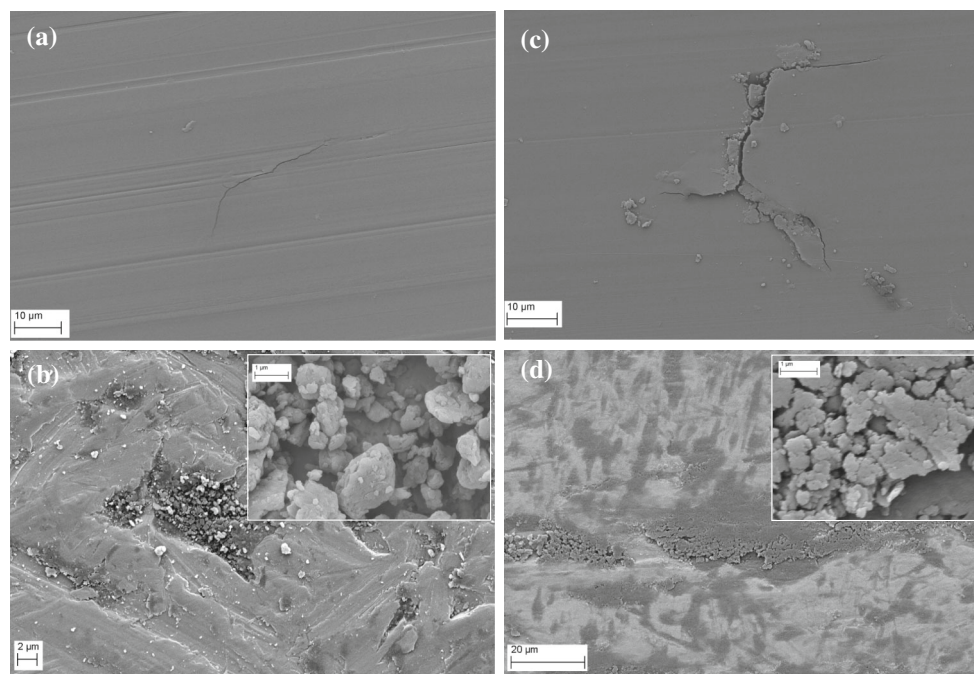


Fig. 15 SEM images of **a** the worn surfaces of PBI, **b** the formation of the TFL on the steel counterpart after 20 min, **c** the worn surfaces of PBI, **d** the formation of the TFL on the steel counterpart after 2 h

TFLs, the wear process is normally governed by mild abrasion wear, i.e. the material removal occurs mainly at the surface of the specimen by cutting and/or ploughing process caused by the hard asperities of the steel counterface. For polymers in abrasive wear, Czichos [21] correlated wear rate to the hardness and yield stress based on Archard model [30], i.e.

$$\Delta V = kA_r L \quad (4)$$

where ΔV is the wear volume, and L is the sliding distance. A_r is the real contact area which is inversely proportional to the hardness. k is defined as the probability of debris particle formation, which can be calculated by the ratio between the actual interfacial stress and the tensile yield stress of the polymer. Since the interfacial stress is mostly determined by the friction coefficient and hardness is normally proportional to the yield stress, the correlation can be simplified as,

$$W_s \sim \frac{\mu}{\sigma^2} \quad (5)$$

Here, W_s is the specific wear rate, μ is the friction coefficient, and σ is the tensile yield stress. This is similar to the well-known Ratner–Lancaster correlation [2, 19, 20]. The later also considered the effect of elongation to break, i.e. the work to rupture determined by the product of stress and strain at rupture was used as damage criterion for the relationship.

Figure 16 compares the specific wear rate of two polymers against μ/σ^2 , which mainly concerns the relationship between wear loss and the mechanical properties of the bulk materials, especially the yield behaviour at different temperatures. In addition, the effect of the TFL on the wear

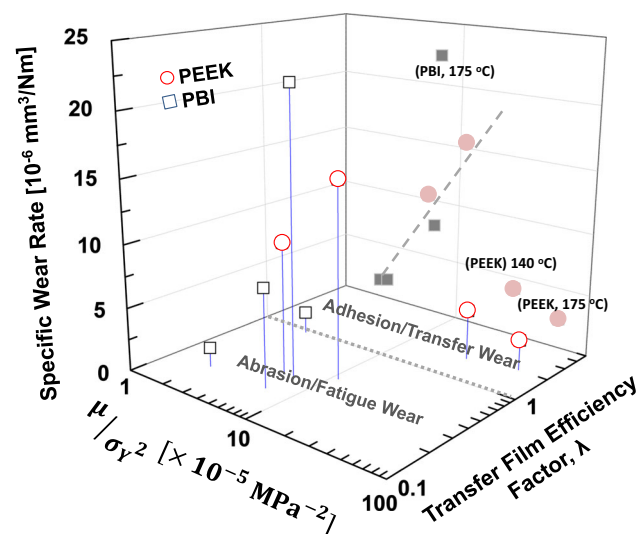


Fig. 16 Dependence of the specific wear rate, w_s on μ/σ^2 and λ . μ friction coefficient; σ tensile yield stress; λ transfer film efficient factor. The solid dots are the projections on μ/σ^2-w_s

rate was illustrated by using the transfer film efficiency factor, λ . A reasonably good correlation between w_s and μ/σ^2 can be seen at relatively low temperatures. However, when sliding condition becomes more severe, PBI showed a much higher wear rate than the values predicted from the linear relationship between W_s and μ/σ^2 . This can be explained by the fracture behaviour of the rigid, brittle PBI. As aforementioned, Eq. (5) was established on the basis of Archard model by assuming that the wear loss was resulted from the cutting/ploughing process by individual asperity tips, depending on the hardness and/or rupture property of the specimen. However, when brittle fracture and crack growth occur, the wear process can be significantly accelerated. Larger particulate wear debris can be formed as the crack length can be much greater than the size of asperities contacts [2, 26]. In particular, where the depth of deformation exceeds some critical value, cracking and fracture may occur on a macro-scale [26, 39], which was also noticed for PBI specimens at high temperatures.

When polymers, on the other hand, show more ductility, the wear mechanism may change into adhesion and transfer wear, with the formation of a continuous, uniform TFL on the counterface, especially when λ is clearly larger than 1. In general, the formation of the TFL may reduce or increase the friction/wear, depending on the properties of the TFL such as surface energy, crystalline structure, and morphology [3, 15, 40–42]. In our case, the friction force was increased due to the strong cohesive force between the polymeric TFL and polymer specimen at high temperatures. However, a low wear rate was achieved within this regime, thanks to the back-transfer of wear debris. During the steady wear stage, the wear debris could be trapped in the wear region and transferred back on the worn surface of the specimen, resulting in a low wear loss of the sliding system. From an energy point of view, the wear-related friction energy is mainly consumed by the transformation of wear debris between contact surfaces, and thus the overall material removal rate is low. Thus, PEEK showed a much lower wear rate than the values predicted from the linear relationship between W_s and μ/σ^2 at high temperatures.

5 Conclusions

The wear behaviour of PEEK and PBI was investigated at room and elevated temperatures. Thanks to its excellent thermal mechanical properties, PBI could achieve a high wear resistance when temperature was lower than 140 °C. However, PEEK showed better wear resistance than PBI when temperature is even higher, despite of the degradation of its mechanical properties. The low wear rate was explained by the change in wear mechanism with the

formation of an effective TFL. In particular, it is noticed that the TFL could transfer back on to the polymer specimen. The process eventually contributed to a low wear loss of the sliding system since the wear debris was effectively trapped in the contact region. The results affirmed the fact that wear is not an intrinsic material property but system behaviour. Under different contact conditions, the tribological properties of polymers could be influenced by the different combinations of properties such as hardness, fracture, and ductility behaviour. In practice, it is important to identify those mechanical properties which are of most significance in wear and thus to select polymer materials as the sliding components for particular circumstances or contact conditions.

Acknowledgements This research was partly supported by the Faculty of Engineering and Information Technologies, the University of Sydney, under the Faculty Research Cluster Program. G. Zhang acknowledges the Chinese “Thousand Youth Talents Plan” for supporting his research work. Authors are greatly indebted to Prof Klaus Friedrich for fruitful discussions and valuable suggestions during the preparation of this paper.

References

- Lancaster, J.K.: Abrasive wear of polymers. *Wear* **14**(4), 223–239 (1969)
- Briscoe, B.: Wear of polymers: an essay on fundamental aspects. *Tribol. Int.* **14**(4), 231–243 (1981)
- Tanaka, K.: Transfer of semicrystalline polymers sliding against a smooth steel surface. *Wear* **75**(1), 183–199 (1982)
- Vaziri, M., Spurr, R.T., Stott, F.H.: An investigation of the wear of polymeric materials. *Wear* **122**(3), 329–342 (1988)
- Santner, E., Czichos, H.: Tribology of polymers. *Tribol. Int.* **22**(2), 103–109 (1989)
- Myshkin, N.K., Petrokovets, M.I., Kovalev, A.V.: Tribology of polymers: adhesion, friction, wear, and mass-transfer. *Tribol. Int.* **38**(11–12 Spec. Iss.), 910–921 (2005)
- Friedrich, K., Chang, L., Hauptert, F.: Current and future applications of polymer composites in the field of tribology. In: Nikolais, L., Meo, M., Milella, E. (eds.) *Composite Materials: A Vision for the Future*, pp. 129–167. Springer, Berlin (2011)
- Briscoe, B., Sinha, S.: Tribological applications of polymers and their composites: past, present and future prospects. In: Friedrich, Klaus, Schlarb, Alois K. (eds.) *Tribology of Polymeric Nanocomposites: Friction and Wear of Bulk Materials and Coatings*, 2nd edn, pp. 1–22. Butterworth Heinemann, Oxford (2013)
- Myshkin, N., Kovalev, A., Spaltman, D., Woydt, M.: Contact mechanics and tribology of polymer composites. *Appl. Polym. Sci.* **131**(3), 39870 (2014)
- Friedrich, K., Lu, Z., Hager, A.M.: Recent advances in polymer composites’ tribology. *Wear* **190**(2), 139–144 (1995)
- Lu, Z.P., Friedrich, K.: On sliding friction and wear of PEEK and its composites. *Wear* **181–183**(2), 624–631 (1995)
- Hanchi, J., Eiss Jr., N.S.: Dry sliding friction and wear of short carbon-fiber-reinforced polyetheretherketone (PEEK) at elevated temperatures. *Wear* **203–204**, 380–386 (1997)
- Samyn, P., Quintelier, J., De Baets, P., Schoukens, G.: Characterisation of polyimides under high-temperature. *Mater. Lett.* **59**(22), 2850–2857 (2005)
- Chang, L., Zhang, Z., Ye, L., Friedrich, K.: Tribological properties of high temperature resistant polymer composites with fine particles. *Tribol. Int.* **40**(7), 1170–1178 (2007)
- Zhang, G., Yu, H., Zhang, C., Liao, H., Coddet, C.: Temperature dependence of the tribological mechanisms of amorphous PEEK under dry sliding conditions. *Acta Mater.* **56**(10), 2182–2190 (2008)
- Pei, X., Friedrich, K.: Sliding wear properties of PEEK, PBI and PPP. *Wear* **274–275**, 452–455 (2012)
- Friedrich, K., Sue, H.J., Liu, P., Almajid, A.A.: Scratch resistance of high performance polymers. *Tribol. Int.* **44**(9), 1032–1046 (2011)
- Häger, A.M., Davies, M.: Short-fibre reinforced, high-temperature resistant polymers for a wide field of tribological applications. In: Friedrich, K. (ed.) *Advanced in Composites Tribology, Composite Materials Series*, vol. 8, pp. 107–157. Elsevier, Amsterdam (1993)
- Lancaster, J.K.: Relationships between the wear of polymers and their mechanical properties. In: 7th. Tribology Group Conv., Paper 12, Gothenburg, 1969. *Inst. Mech. Engrs.*, London (1969)
- Ratner, S.B., Farberova, I.I., Radyukevich, O.V., Lure, E.G.: Connection between the wear resistance of plastics and other mechanical properties. *Sov. Plast.* **7**, 37 (1964)
- Czichos, H.: Influence of adhesive and abrasive mechanisms on the tribological behaviour of thermoplastic polymers. *Wear* **88**(1), 27–43 (1983)
- Häger, A.M., Friedrich, K., Junghans, R.: Selected thermoplastic bearing materials for use at elevated temperatures. *Wear* **162–164**, 649–655 (1993)
- Marx, S., Junghans, R.: Friction and wear of highly stressed thermoplastic bearings under dry sliding conditions. *Wear* **193**(2), 253–260 (1996)
- Lu, Y., Chen, J., Cui, H., Zhou, H.: Mechanical and tribological properties of titanium reinforced polybenzimidazole. *Proc. Inst. Mech. Eng. Part J: J. Eng. Tribol.* **223**(7), 971–975 (2009)
- Sharma, S., Padenko, E., Bijwe, J., Wetzel, B., Friedrich, K.: Erosive and sliding wear of polybenzimidazole at elevated temperatures. *J. Mater. Sci.* **51**(1), 262–270 (2015)
- Lancaster, J.K.: Material-specific wear mechanisms: relevance to wear modelling. *Wear* **141**(1), 159–183 (1990)
- Chang, L., Friedrich, K., Ye, L.: Study on the transfer film layer in sliding contact between polymer composites and steel disks using nanoindentation. *J. Tribol.* **136**(2), 021602 (2014)
- Karger-Kocsis, J., Friedrich, K.: Temperature and strain-rate effects on the fracture toughness of poly(ether ether ketone) and its short glass-fibre reinforced composite. *Polymer* **27**(11), 1753–1760 (1986)
- Häger, A.M.: Polyaryletherketone für den einsatz in gleitlagern und gleitelementen. Ph.D. Thesis, TU Kaiserslautern (1996). ISBN 3-8365-2094-7
- Archard, J.F.: Contact and rubbing of flat surfaces. *J. Appl. Phys.* **24**(8), 981–988 (1953)
- Zhang, G., Schlarb, A.K.: Correlation of the tribological behaviours with the mechanical properties of poly-ether-ether-ketones (PEEKs) with different molecular weights and their fiber filled composites. *Wear* **266**(1–2), 337–344 (2009)
- Dubourg, M.C., Chateauinois, A., Villechaise, B.: In situ analysis and modeling of crack initiation and propagation within model fretting contacts using polymer materials. *Tribol. Int.* **36**, 109–119 (2003)
- Li, F., Hu, K., Li, J., Zhao, B.: The friction and wear characteristics of nanometer ZnO filled polytetrafluoroethylene. *Wear* **249**, 877–882 (2002)
- Yang, E.-L., Hirvonen, J.-P., Toivanen, R.O.: Effect of temperature on the transfer film formation in sliding contact of PTFE with stainless steel. *Wear* **146**(2), 367–376 (1991)

35. Bahadur, S.: The development of transfer layers and their role in polymer tribology. *Wear* **245**, 92–99 (2000)
36. Randall, N.X., Harris, A.: Nanoindentation as a tool for characterizing the mechanical properties of tribological transfer films. *Wear* **245**(1), 196–203 (2000)
37. Chang, L., Zhang, Z., Ye, L., Friedrich, K.: Tribological properties of epoxy nanocomposites: III characteristics of transfer film. *Wear* **262**, 699–706 (2007)
38. Briscoe, B.J., Sinha, S.K.: Wear of polymers. *Proc. Inst. Mech. Eng. Part J: J. Eng. Tribol.* **216**(6), 401–441 (2002)
39. Atkins, A.G., Mai, Y.W.: *Elastic and Plastic Fracture*. Ellis Horwood, Chichester (1985)
40. Uruena, J.M., Pitenis, A.A., Harris, K.L., Sawyer, W.G.: Evolution and wear of fluoropolymer transfer films. *Tribol. Lett.* **57**, 9 (2015)
41. Li, H.L., Yin, Z.W., Jiang, D., Jin, L.Y., Cui, Y.Q.: A study of the tribological behaviour of transfer films of PTFE composites formed under different loads, speeds and morphologies of the counterface. *Wear* **328–329**, 17–27 (2015)
42. Ye, J., Moore, A.C., Burris, D.L.: Transfer film tenacity: a case study using ultra-low-wear alumina—PTFE. *Tribol. Lett.* **59**, 50 (2015)